SCIENCE CHINA
Chemistry

•ARTICLES•

https://doi.org/10.1007/s11426-019-9606-2

Enantioselective three-component Ugi reaction catalyzed by chiral phosphoric acid

Jian Zhang[1,2], Yi-Yan Wang[2], He Sun[2], Shao-Yu Li[2,3], Shao-Hua Xiang[2,3] & Bin Tan[2*]

[1]*School of Chemistry and Chemical Engineering, Harbin Institute of Technology, Harbin 150001, China;*
[2]*Department of Chemistry and Shenzhen Grubbs Institute, Southern University of Science and Technology, Shenzhen 518055, China;*
[3]*Academy for Advanced Interdisciplinary Studies, Southern University of Science and Technology, Shenzhen 518055, China*

Received July 31, 2019; accepted September 5, 2019; published online October 22, 2019

A catalytic enantioselective three-component Ugi reaction was developed. SPINOL-derived phosphoric acid with bulky 2,4,6-tricyclohexylphenyl groups at the 6,6′ positions was found to be the best catalyst to afford α-amino amide derivatives in good to excellent yields (62% to 99%) and enantiocontrol (81% to >99% enantiomeric excess). This asymmetric reaction was applicable well to an array of aliphatic aldehydes. The gram-scale synthesis, modification of dapsone, and enantioselective synthesis of (*R*)-Lacosamide underline the general utility of this methodology. Influence of dihedral angles and substituents of the chiral phosphoric acids on the enantioselectivity was also discussed in this article.

α-amino amide, Ugi reaction, chiral phosphoric acid, enantioselectivity, Lacosamide

Citation: Zhang J, Wang YY, Sun H, Li SY, Xiang SH, Tan B. Enantioselective three-component Ugi reaction catalyzed by chiral phosphoric acid. *Sci China Chem*, 2019, 62, https://doi.org/10.1007/s11426-019-9606-2

1 Introduction

The amide is one of the most basic functional groups that constitute organic compounds. Amidation is the major reaction for peptide and protein synthesis from its fundamental building blocks α-amino acids (Figure 1(a)) [1–3]. α-Amino amides, derivatives of α-amino acids from amidation with amines, represent ubiquitous subunits that occur in biologically active compounds (Figure 1(b)) [4,5], natural products (Figure 1(b)) [6], and drugs (Figure 1(c)) [7]. Besides as building blocks, α-amino amides have been developed as ligands [8,9], catalysts [10], and co-catalysts [11] (Figure 1(d)). Technical innovations such as chirality analysis [12], ion recognition [13], and fluorescent detection [14] based on α-amino amides have also been reported. The predominant and conventional synthetic route to α-amino amides is amidation of N-protected amino acids with amines (Figure 1(f), right) [15,16]. However, this strategy suffers from several drawbacks, such as the waste generated from the use of expensive coupling reagents, the low efficiency caused by protection and deprotection steps, the epimerization of sensitive α-chiral acids through the formation of oxazolone intermediates, and the limitation of commercial α-amino acids for structural modification [17,18]. Thus, catalytic and highly enantioselective methods for the diverse synthesis of α-amino amides are still in great demands.

Multicomponent reactions (MCRs) [19] are developed toward the goal of "ideal synthesis" [20] with high atom economy and efficiency, as well as high molecular complexity and product diversity [21]. Ugi reaction is a representative MCR which has been used widely [22] in organic synthesis, polymer engineering, and drug discovery. Generally, Ugi reaction is the one-pot reaction of an amine, a carbonyl compound, an isocyanide, and an acid component ((Figure 1(e)). The key intermediate of Ugi reaction is commonly considered to be a nitrilium ion, which is resulted

*Corresponding author (email: tanb@sustech.edu.cn)

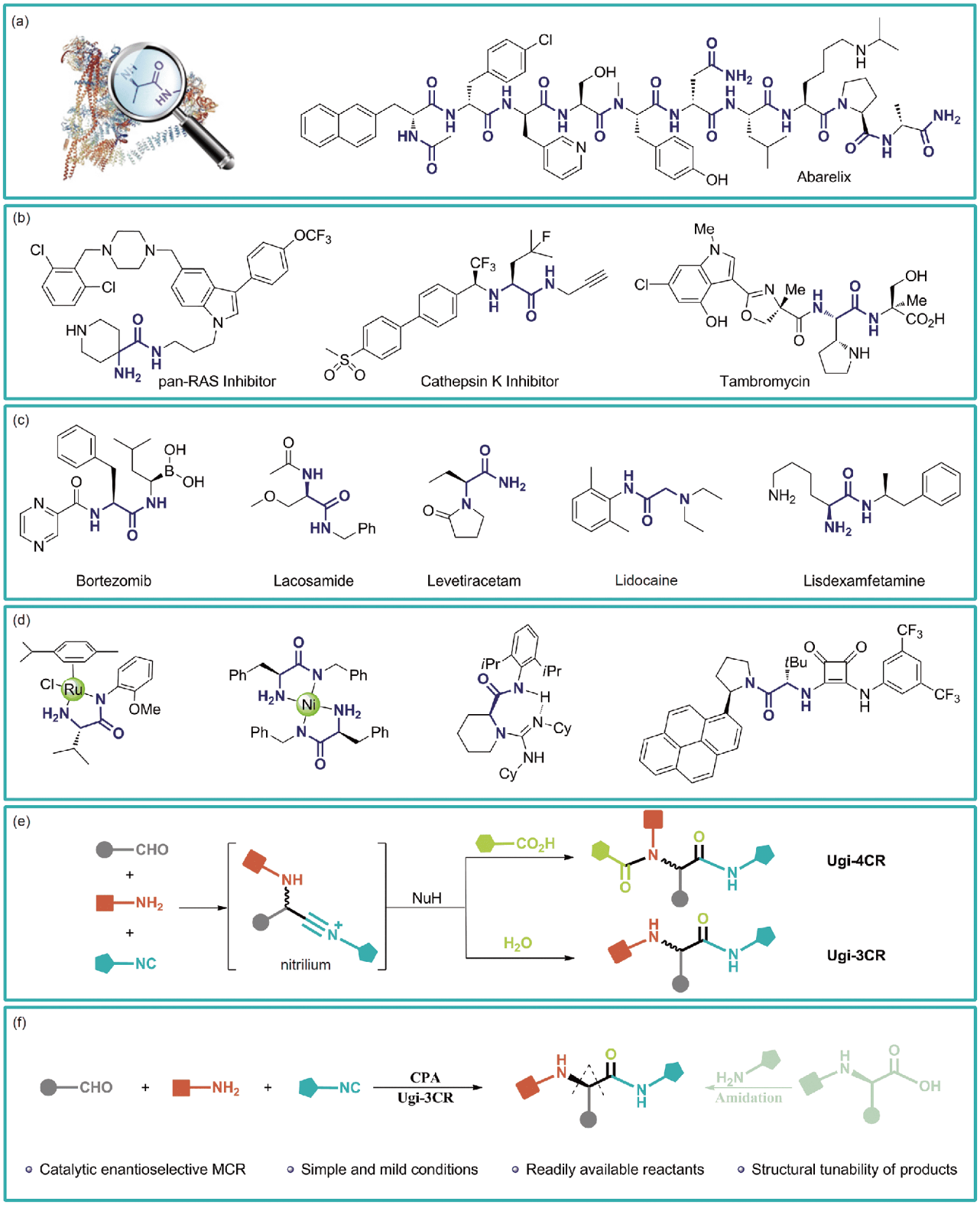

Figure 1 (a) Cryo-EM structure of the catalytically activated yeast spliceosome (B*-a1 complex) and marketed peptide drug Abarelix; (b) bioactive molecules and natural product Tambromycin; (c) top-selling drugs with α-amino amide moiety in recent years; (d) α-amino amides used as ligands and catalysts in organic synthesis; (e) Ugi-4CR and Ugi-3CR; (f) enantioselective Ugi-3CR versus amidation for the synthesis of α-amino amides (color online).

from α-addition of the isocyanide to the *in situ* generated imine. The nitrilium ion can be trapped by many kinds of nucleophilic components [23], such as carboxylic acids and water. Trapped by a carboxylic acid, the nitrilium ion con-

verts to an imidate which undergoes Mumm rearrangement to form an α-acylamino amide. Such a transformation is the prototypical four-component Ugi reaction (Ugi-4CR) [24]. Alternatively, when trapped by water, the nitrilium ion coverts to an α-amino amide derivative. Such a process is commonly named as three-component Ugi reaction (Ugi-3CR) which was firstly developed by List *et al.* [25].

In light of the importance of α-amino amides and the advantages of MCRs, the pursuit of a mild, simple, highly enantioselective Ugi-3CR with commercially available starting materials is highly desirable (Figure 1(f), left). The structures of the α-amino amides formed via Ugi-3CR are more tunable compared to those made by the conventional amidation strategy, as the former is based on three achiral building blocks while the latter relies on the ready-made chiral α-amino acids. In addition, enantioselective Ugi-3CR offers facile delivery of distinct stereoisomers by judicious choice of the catalyst configuration. The diversity of structures and the controllability of stereochemistry are necessary for biological activity studies [26], drug development [27] and catalyst modifications [28].

Despite some advances have been made in enantioselective α-addition of isocyanides [29–31], the development of catalytic asymmetric Ugi reactions is greatly lagged due to the complex reaction system, the competing reactions, and the difficulty in the enantiocontrol of the α-addition of isocyanides. A catalytic enantioselective Ugi-type reaction was firstly introduced in 2009 by Zhu and co-workers [32,33]. After that, only limited examples of enantioselective Ugi reactions have been reported. Maruoka and co-workers [34] developed a chiral dicarboxylic acid-catalyzed Ugi-type reaction with acyclic azomethine imines. Wang, Zhu, and co-workers [35] reported a catalytic asymmetric four-center three-component Ugi reaction by dynamic kinetic resolution of the primary multicomponent adduct. In all cases mentioned above, transient nitrilium intermediates were trapped by internal oxygens. Particularly worth to mention is that Wulff and co-workers [36] successfully developed an asymmetric Ugi-3CR enabled by an elegantly designed BOROX catalyst that was assembled *in situ* from a chiral biaryl ligand, an amine, water, $BH_3{\cdot}SMe_2$, and an alcohol (or phenol) to afford α-amino amides. Nonetheless, this enantioselective Ugi-3CR protocol is restricted to aromatic aldehydes, and the extension to aliphatic aldehydes remains challenging. Recently, our group [37] reported a catalytic asymmetric Ugi-4CR in which direct enantiocontrol of the α-addition of isocyanides with activated imines as electrophiles and external carboxylic acids as nucleophiles was fulfilled. As our continuous research interest in asymmetric MCRs [37–40], we aimed to develop an asymmetric Ugi-3CR with complementary substrate scope, as aliphatic aldehydes derived α-amino amides are more common in naturally occurring compounds and drugs. Usually, Ugi-3CR proceeds with acid catalysis by lowering the lowest unoccupied molecular orbital (LUMO) energies of the imines [25,41,42]. Therefore, we envision that a chiral phosphoric acid (CPA) [43,44] might enable aliphatic aldehydes to function as feasible substrates for enantioselective Ugi-3CR. Rapid imine formation, as well as its preferential activation over the carbonyl group, are viable with a CPA catalyst to suppress competing reactions such as the Passerini-type reaction [29]. Suitable interactions between a bulky CPA and the small substrates may lead to the improvement of enantioselectivity for the less sterically hindered aldehydes [45].

2 Results and discussion

After some initial trials (Table S2, Supporting Information online), we set out to optimize the model catalytic asymmetric Ugi-3CR of 2-benzyloxy acetaldehyde (**1a**), 4-nitroaniline (**2a**), and cyclohexyl isocyanide (**3a**) in CH_2Cl_2 at −30 °C (Table 1). The BINOL-derived **CPA1** and **CPA2** gave moderate yields and low enantioselectivities (Table 1, entries 1, 2). By tuning the substituents on 3,3′ positions of the BINOL skeleton, we found that more steric hindrance led to the improvement of enantioselectivity. **CPA3** with 2,4,6-triisopropylphenyl substituents provided a 40% enantiomeric excess (*ee*) (entry 3), and bulkier 2,4,6-tricyclohexylphenyl substituted **CPA4** boosted the enantioselectivity to 81% *ee* (entry 4). The CPA with 9-anthryl as substituents (**CPA5**) catalyzed the reaction in 24% yield with 7% *ee* (entry 5). Then we turned to the SPINOL-derived CPAs. The negligible difference in enantioselectivity was detected for **CPA6** and **CPA1** despite the different chiral skeletons (entries 1, 6). A slight increase in enantioselectivity was found when catalyst changes from **CPA2** to **CPA7** (entries 2, 7). Notably, a dramatic improvement was observed when **CPA8** (88% *ee*) was employed (entry 8). The enantiocontrol was further enhanced (97% *ee*) when the reaction was facilitated by **CPA10**; meanwhile, the best yield (72%) was achieved among all the catalysts (entries 1–10). Attempts to further improve the chemical yield upon evaluation of various solvents (entries 11–14) and temperatures (entries 15, 16) met with failure. Finally, the yield increased to 91% (entry 17) when excess aldehyde was added and the reaction time was prolonged.

Having established the optimum conditions, the scope and limitation of this reaction were evaluated by exploring different reaction components (Table 2). The reaction was applicable well to an array of linear aliphatic aldehydes which gave moderate enantioselectivity in previous Ugi-type reaction [32]. For acetaldehyde (**5**), a very small substrate, an 84% yield with 87% *ee* was obtained. Besides, the length of the substitutions on the aldehydes was well-tolerated, as

Table 1 Optimization of reaction conditions [a)]

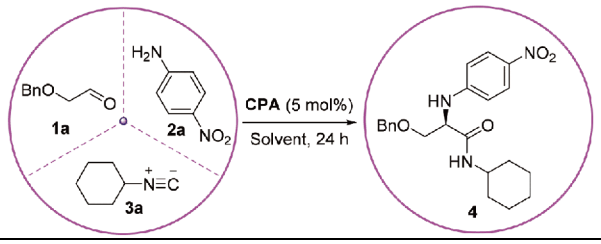

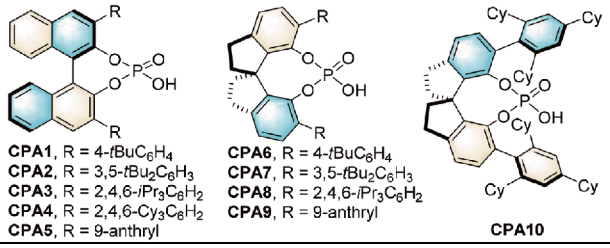

Entry	CPA	Solvent	*T* (°C)	Yield (%) [b)]	*ee* (%) [c)]
1	**CPA1**	CH_2Cl_2	−30	40	−15 [d)]
2	**CPA2**	CH_2Cl_2	−30	41	−18 [d)]
3	**CPA3**	CH_2Cl_2	−30	54	40
4	**CPA4**	CH_2Cl_2	−30	61	81
5	**CPA5**	CH_2Cl_2	−30	24	7
6	**CPA6**	CH_2Cl_2	−30	47	14
7	**CPA7**	CH_2Cl_2	−30	50	−32 [d)]
8	**CPA8**	CH_2Cl_2	−30	55	−88 [d)]
9	**CPA9**	CH_2Cl_2	−30	36	−35 [d)]
10	**CPA10**	CH_2Cl_2	−30	72	97
11	**CPA10**	$CHCl_3$	−30	43	95
12	**CPA10**	Et_2O	−30	18	86
13	**CPA10**	EtOAc	−30	19	87
14	**CPA10**	Toluene	−30	41	96
15	**CPA10**	CH_2Cl_2	−10	74	96
16	**CPA10**	CH_2Cl_2	30	49	90
17 [e)]	**CPA10**	CH_2Cl_2	−30	91	97

a) Unless otherwise specified, the reaction of **1a** (0.05 mmol), **2a** (0.05 mmol), **3a** (0.05 mmol), and catalyst (5 mol%), was carried out in 1 mL of CH_2Cl_2; b) isolated yield; c) determined by HPLC analysis; d) negative ee refers to the inverted configuration of the more abundant product enantiomer; e) **1a** (0.2 mmol), **2a** (0.1 mmol), **3a** (0.1 mmol), and catalyst (5 mol%) was carried out in 2 mL of CH_2Cl_2, 36 h.

ethyl (**6**), *n*-propyl (**7**), *n*-butyl (**8**), and *n*-pentyl (**9**) groups all gave excellent enantioselectivities (91% to 94% *ee*). A thioether substituent (**10**) was also compatible with this reaction to afford the corresponding product in 91% *ee*. Both 3-phenylpropanal (**11**) and 2-phenylacetal (**12**) furnished the desired products in excellent yields (90% and 96%, respectively) and good enantioselectivities (93% *ee* and 83% *ee*, respectively). The diminished enantioselectivity for the latter may result from the absence of oxygen on the chain and the increase of the steric encumbrance. Similarly, isovaleraldehyde (**13**) and isobutyraldehyde (**14**) gave rise to products with decreased enantioselectivities (85% *ee* and 81% *ee*, respectively). A symmetrical dialdehyde (**15**) with a central *N*-*tert*-butyloxycarbonyl group underwent a dual reaction at both carbonyls with a 13:1 diastereomeric ratio (d.r.) and >99% *ee*. Electronic and position variations in the aryl ring of the anilines were also examined. Reactants with electron-withdrawing (strong to moderate) substituents on the *para* positions (**16**–**20**), *meta*-nitro substituent (**21**), multiple substituents (**22**, **23**), and neutral substituent (**24**) all reacted in high yields (87% to 99%) and excellent enantioselectivities (92% to 98% *ee*). In addition, a β-naphthylamine derivative formed product **25** in almost quantitative yield with 96% *ee*. A dual reaction at both amino groups of dapsone (**26**) [46], an antileprosy medicine, provided an effective method for stereoselective (>20:1 d.r., >99% *ee*) modification of pharmaceuticals. Unfortunately, the use of aromatic aldehydes or aliphatic amines met with failure under current optimal conditions, giving Ugi products in very low yields (Table S3). The steric encumbrance of substituents on isocyanides has only negligible effects on the reaction, as *n*-butyl (**27**), cyclopentyl (**28**), *t*-butyl (**29**), and 1,1,3,3-tetramethyl butyl (**30**) groups all led to good yields (86% to 96%) and excellent enantioselectivities (97% to 98% *ee*). Besides, *p*-methoxyphenyl isonitrile was also amenable to this reaction, producing **31** in 86% yield and 96% *ee*.

To evaluate the general utility of the protocol, we performed a gram-scale reaction. Compound **4** (Figure 2(a)) was produced in 92% yield (1.46 g) and 97% *ee* under the standard conditions. To further illustrate the potential application of our method, we conducted the enantioselective synthesis

Table 2 substrate scope [a)]

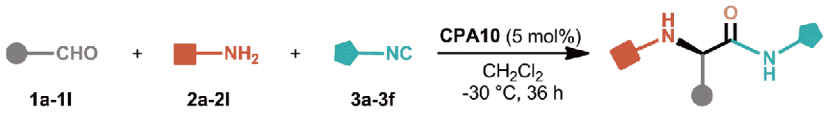

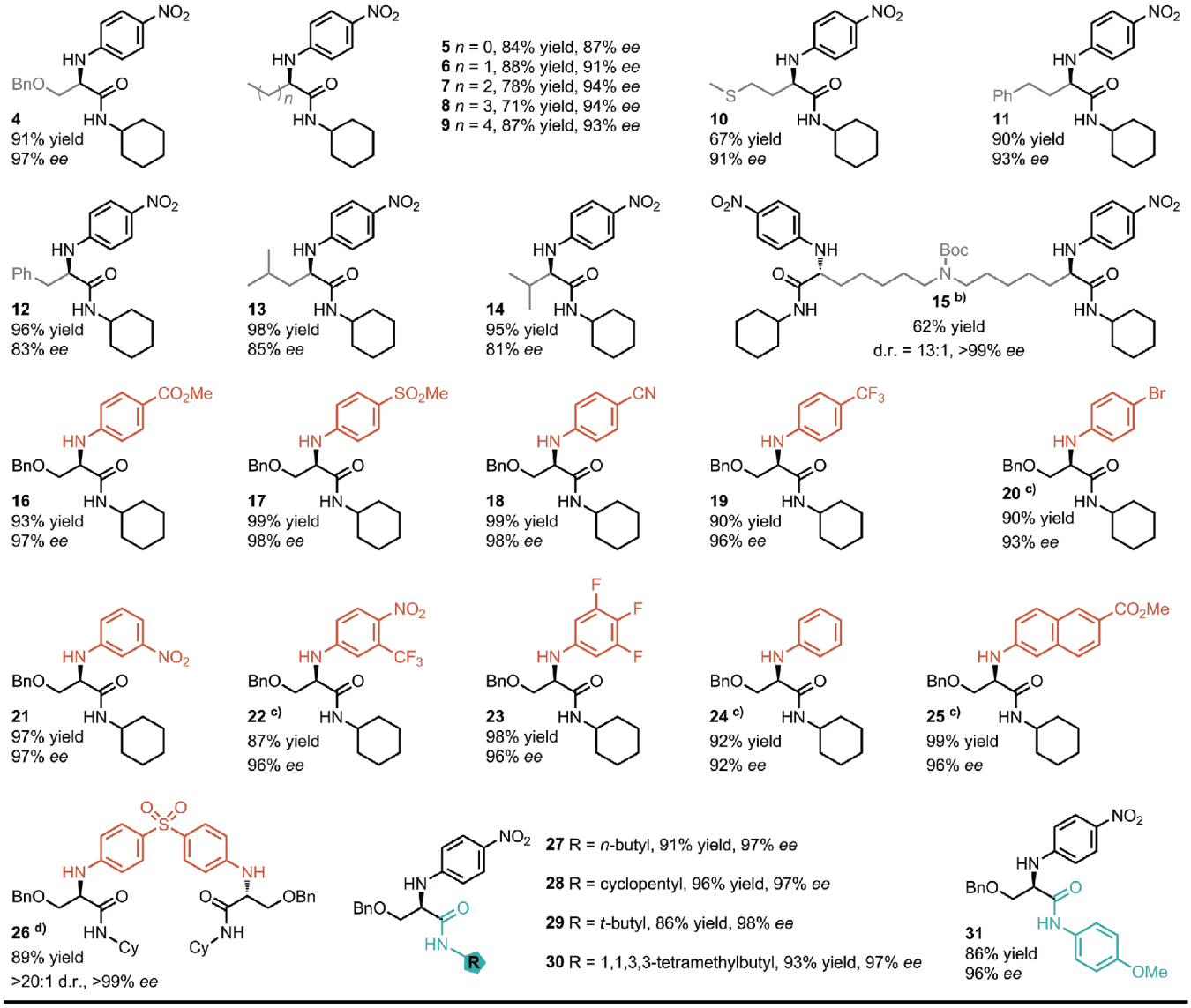

a) Unless otherwise specified, the reaction of **1** (0.2 mmol), **2** (0.1 mmol), **3** (0.1 mmol), and catalyst (5 mol%) was carried out in 2 mL of CH_2Cl_2, isolated yields were gave; b) **1** (0.1 mmol), **2** (0.2 mmol), **3** (0.2 mmol); c) **1** (0.2 mmol), **2** (0.2 mmol), **3** (0.1 mmol); d) **1** (0.2 mmol), **2** (0.1 mmol), **3** (0.2 mmol).

of the anticonvulsive drug (*R*)-Lacosamide [47] via asymmetric Ugi-3CR [48] (Figure 2(b)). The reaction of 2-methoxy acetaldehyde (**1m**), 4-nitroaniline (**2a**), and benzyl isocyanide (**3g**) afforded Ugi product **32** in 90% yield and 94% *ee*. Recrystallization gave rise to a product of higher enantiopurity (>99% *ee*), which delivered **33** in 95% yield after dearylation via sequential reduction and oxidation. Acylation of the chiral amine **33** formed **34** in 88% yield and 96% *ee*. The absolute configuration of **34**, by which the configurations of **4**–**32** can be deduced, is matched with commercial (*R*)-Lacosamide by comparing its high performance liquid chromatography (HPLC) spectrum. Finally, (*R*)-Lacosamide (99.9% *ee*) was obtained in 44% overall yield via three steps of reaction and two steps of recrystallization.

The proposed mechanism is shown in Scheme 1. Initially, the condensation of an amine and an aldehyde affords an imine which will be subsequently activated by CPA via a hydrogen bond. There may be two bonding models for different imines. Imines with an oxygen atom in the substituent chain (**4**, **16**–**32**) may take model 1 while imines without an oxygen atom in the substituent chain (**5**–**15**) may take model

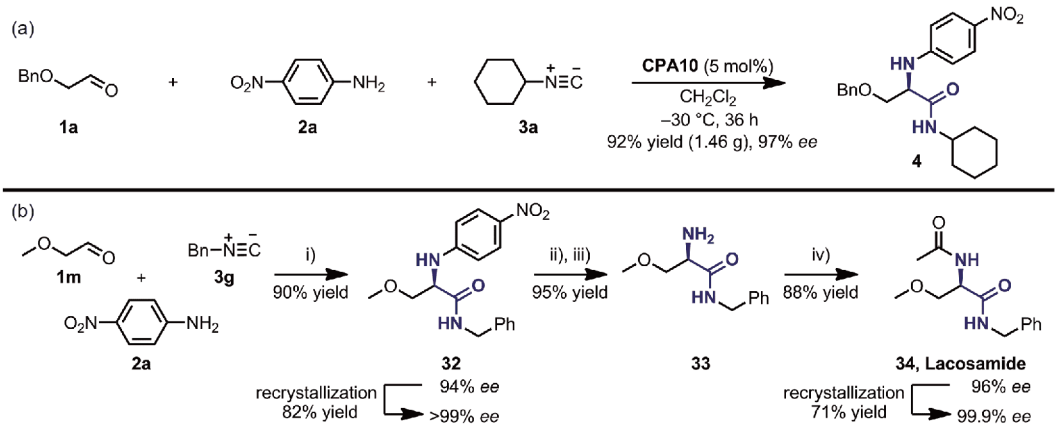

Figure 2 (a) Gram-scale synthesis of **4**; (b) enantioselective synthesis of (*R*)-Lacosamide via Ugi-3CR. i) 5 mol% **CPA10**, CH_2Cl_2/H_2O, r.t., 8 h; ii) H_2 (1 atm), 5 mol% Pd/C, EtOAc, r.t., 4 h; iii) $PhI(OAc)_2$, MeCN, 0 °C, 30 min, then 1 M H_2SO_4, r.t., 1 h; iv) Ac_2O, pyridine, THF, r.t., 1 h (color online).

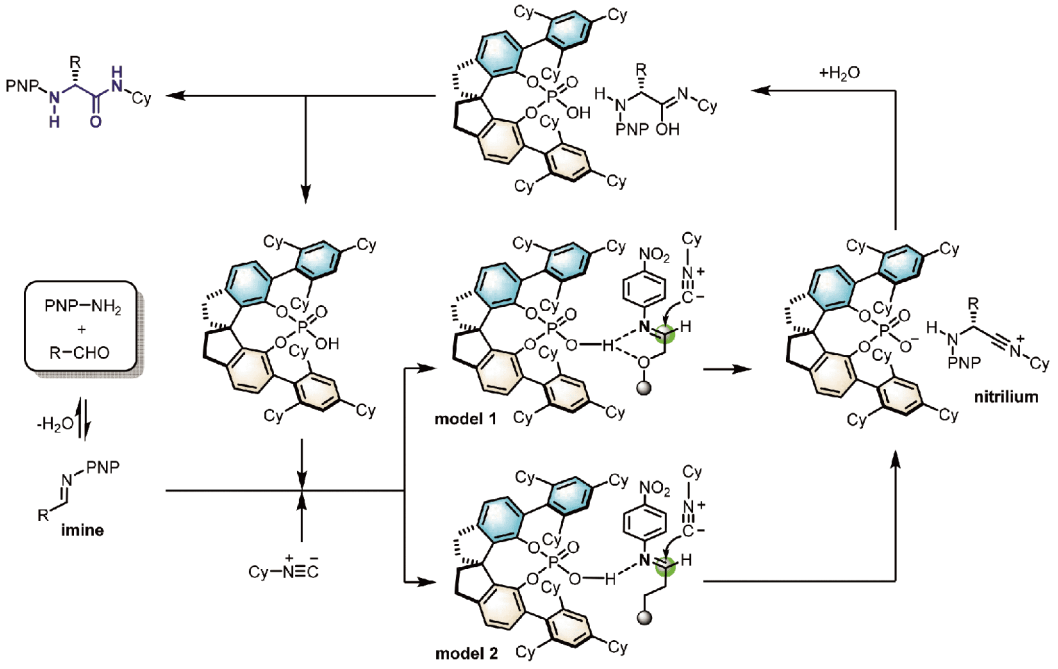

Scheme 1 Proposed mechanism for chiral phosphoric acid-catalyzed enantioselective Ugi-3CR. PNP, *p*-nitrophenyl (color online).

2, as the oxygen can contact with the hydrogen and thus strengthen the rigidity of the interaction between the catalyst and substrates to give enhanced enantioselectivities. The activated imine is then subjected to nucleophilic attack by the isocyanide, which leads to the formation of a nitrilium intermediate accompanying with the chiral phosphate anion. Trapping by water, the nitrilium converts to the final product via an unstable intermediate while the phosphate anion is protonated to regenerate the CPA.

We tried to understand the enantioselectivity from basic chiral skeletons and substituents of three CPAs. Putting the crystal structure of **CPA3** (Figure 3(a)) [49], **CPA8** (Figure 3(d)) [50], and **CPA10** (Figure 3(g)) into a three-dimensional system of coordinates, and defining the C2-symmetric axis as *Z*-axis while the axis through the two pink carbon atoms as *Y*-axis, views from the C2-symmetric axes of the three different CPAs were obtained. The dihedral angle between aryl ring A and A′ (plane A and plane A′) is 51.5° (Figure 3(b)) in BINOL-derived **CPA3**; while it is 59.4° in SPINOL-derived **CPA8** (Figure 3(e)). This means that **CPA8** has a more stretched structure in the direction of *X*-axis. The dihedral angle between aryl ring B and B′ (plane B and plane B′) in **CPA8** (54.8°, Figure 3(f)) is smaller than that in BINOL-derived **CPA3** (73.5°, Figure 3(c)), reflecting that the former has a more confined structure in the direction of *Y*-axis. This is consistent with the experimentally observed higher en-

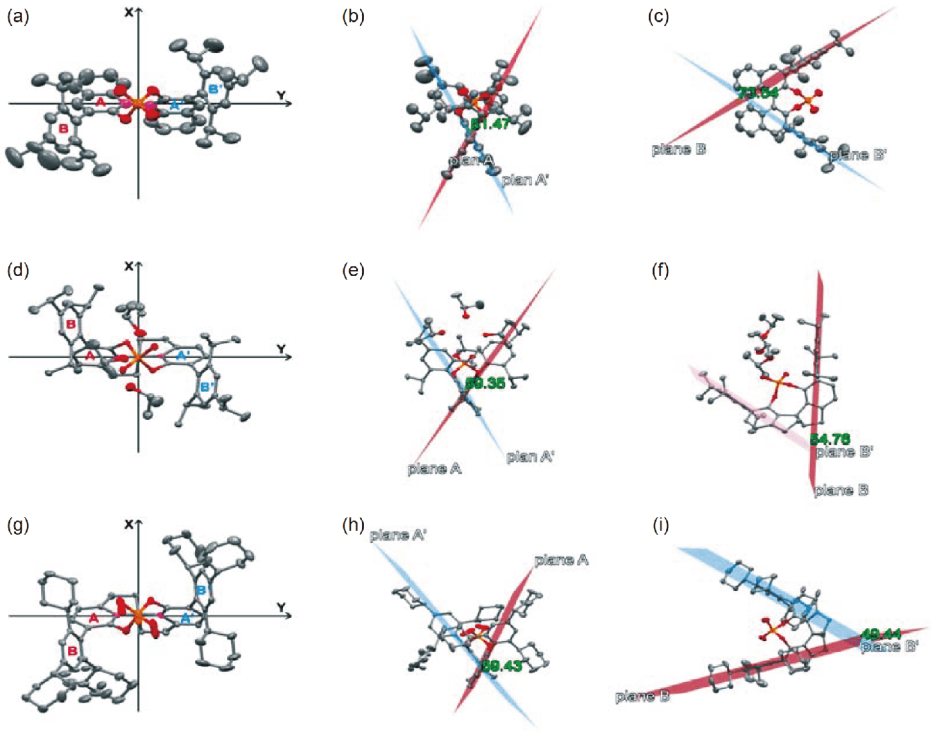

Figure 3 (a) Top view of **CPA3** from *Z*-axis; (b) side view of **CPA3** from *Y*-axis; (c) side view of **CPA3** from *X*-axis; (d) top view of **CPA8** from *Z*-axis; (e) side view of **CPA8** from *Y*-axis; (f) side view of **CPA8** near *X*-axis; (g) top view of **CPA10** from *Z*-axis; (h) side view of **CPA10** from *Y*-axis; (i) side view of **CPA10** near *X*-axis (color online).

antioselectivity using **CPA8** (88% *ee*) as compared to that using **CPA3** (40% *ee*). Both dihedral angles between aryl ring A and A′ (plane A and plane A′) of **CPA8** (Figure 3(e)) and of **CPA10** (Figure 3(h)) are 59.4°. Replacing of the *i*-propyl substituents (Figure 3(f)) with cyclohexyl groups (Figure 3(i)) leads to a slight decrease (5.4°) in the dihedral angle between aryl ring B and B′ (plane B and plane B′), and further increases the enantioselectivity (from 88% *ee* to 97% *ee*). Therefore, the hindrance of substituents may be the main factor when comparing **CPA8** with **CPA10** in the enantiocontrol of the reaction.

3 Conclusions

In summary, we have successfully developed a SPINOL-derived phosphoric acid-catalyzed enantioselective three-component Ugi reaction. The reaction is easy to conduct with simple conditions. A series of aliphatic aldehydes, aryl amines, and isocyanides with different steric hindrance are well-tolerated, leading to the formation of α-amino amides in good yields (62% to 99%) and high enantioselectivities (81% to >99% *ee*). Our protocol was proved applicable in gram-scale synthesis. In addition, enantioselective synthesis of antiepileptic agent (*R*)-Lacosamide was accomplished with this asymmetric Ugi-3CR as the key step. While distinct backbone structures of BINOL-derived **CPA3** and SPINOL-derived **CPA8** may account for the difference in enantioselectivity between those two types of catalysts, the hindrance of substituents which leads to different sizes of the catalytic pocket may be the main factor of different enantioselectivities for **CPA8** and **CPA10**.

Acknowledgements This work was supported by the National Natural Science Foundation of China (21825105, 21772081), Shenzhen Special Funds for the Development of Biomedicine, Internet, New Energy, and New Material Industries (JCYJ20170412151701379, KQJSCX20170328153203), Special Funds for the Cultivation of Guangdong College Students' Scientific and Technological Innovation (PDJH2019C467).

Conflict of interest The authors declare that they have no conflict of interest.

Supporting information The supporting information is available online at http://chem.scichina.com and http://link.springer.com/journal/11426. The supporting materials are published as submitted, without typesetting or editing. The responsibility for scientific accuracy and content remains entirely with the authors.

1 Kent SBH. *Chem Soc Rev*, 2009, 38: 338–351
2 D'Hondt M, Bracke N, Taevernier L, Gevaert B, Verbeke F, Wynendaele E, De Spiegeleer B. *J Pharm Biomed Anal*, 2014, 101: 2–30
3 Wan R, Bai R, Yan C, Lei J, Shi Y. *Cell*, 2019, 177: 339–351
4 Welsch ME, Kaplan A, Chambers JM, Stokes ME, Bos PH, Zask A, Zhang Y, Sanchez-Martin M, Badgley MA, Huang CS, Tran TH, Akkiraju H, Brown LM, Nandakumar R, Cremers S, Yang WS, Tong L, Olive KP, Ferrando A, Stockwell BR. *Cell*, 2017, 168: 878–889
5 Mons E, Jansen IDC, Loboda J, van Doodewaerd BR, Hermans J,

Verdoes M, van Boeckel CAA, van Veelen PA, Turk B, Turk D, Ovaa H. *J Am Chem Soc*, 2019, 141: 3507–3514
6 Miley GP, Rote JC, Silverman RB, Kelleher NL, Thomson RJ. *Org Lett*, 2018, 20: 2369–2373
7 McGrath NA, Brichacek M, Njardarson JT. *J Chem Educ*, 2010, 87: 1348–1349
8 Pelagatti P, Carcelli M, Calbiani F, Cassi C, Elviri L, Pelizzi C, Rizzotti U, Rogolino D. *Organometallics*, 2005, 24: 5836–5844
9 Burguete MI, Collado M, Escorihuela J, Luis SV. *Angew Chem Int Ed*, 2007, 46: 9002–9005
10 Yu Z, Liu X, Zhou L, Lin L, Feng X. *Angew Chem Int Ed*, 2009, 48: 5195–5198
11 Banik SM, Levina A, Hyde AM, Jacobsen EN. *Science*, 2017, 358: 761–764
12 Altava B, Burguete MI, Carbó N, Escorihuela J, Luis SV. *Tetrahedron-Asymmetry*, 2010, 21: 982–989
13 Gorla L, Martí-Centelles V, Altava B, Burguete MI, Luis SV. *Dalton Trans*, 2017, 46: 2660–2669
14 Zhang W, Liu F, Zhang C, Luo JG, Luo J, Yu W, Kong L. *Anal Chem*, 2017, 89: 12319–12326
15 Katritzky AR, Mohapatra P. P, Singh S, Clemens N, Kirichenko K. *J Serb Chem Soc*, 2005, 70: 319–327
16 Valeur E, Bradley M. *Chem Soc Rev*, 2009, 38: 606–631
17 Pattabiraman VR, Bode JW. *Nature*, 2011, 480: 471–479
18 Zhu YP, Mampuys P, Sergeyev S, Ballet S, Maes BUW. *Adv Synth Catal*, 2017, 359: 2481–2498
19 Ugi I, Dömling A, Hörl W. *Endeavour*, 1994, 18: 115–122
20 Dömling A, Ugi I. *Angew Chem Int Ed*, 2000, 39: 3168–3210
21 Ruijter E, Scheffelaar R, Orru RVA. *Angew Chem Int Ed*, 2011, 50: 6234–6246
22 Dömling A. *Chem Rev*, 2006, 106: 17–89
23 Ugi I, Steinbrückner C. *Angew Chem*, 1960, 72: 267–268
24 Ugi I, Meyr R, Fetzer U, Steinbrückner C. *Angew Chem*, 1959, 71: 386
25 Pan SC, List B. *Angew Chem Int Ed*, 2008, 47: 3622–3625
26 Tomlin FM, Gerling-Driessen UIM, Liu YC, Flynn RA, Vangala JR, Lentz CS, Clauder-Muenster S, Jakob P, Mueller WF, Ordoñez-Rueda D, Paulsen M, Matsui N, Foley D, Rafalko A, Suzuki T, Bogyo M, Steinmetz LM, Radhakrishnan SK, Bertozzi CR. *ACS Cent Sci*, 2017, 3: 1143–1155
27 Noyori R. *Angew Chem Int Ed*, 2002, 41: 2008–2022
28 Xiao KJ, Lin DW, Miura M, Zhu RY, Gong W, Wasa M, Yu JQ. *J Am Chem Soc*, 2014, 136: 8138–8142
29 Wang Q, Wang DX, Wang MX, Zhu J. *Acc Chem Res*, 2018, 51: 1290–1300
30 Luo W, Yuan X, Lin L, Zhou P, Liu X, Feng X. *Chem Sci*, 2016, 7: 4736–4740
31 Xiong Q, Dong S, Chen Y, Liu X, Feng X. *Nat Commun*, 2019, 10: 2116
32 Yue T, Wang MX, Wang DX, Masson G, Zhu J. *Angew Chem Int Ed*, 2009, 48: 6717–6721
33 Su Y, Bouma MJ, Alcaraz L, Stocks M, Furber M, Masson G, Zhu J. *Chem Eur J*, 2012, 18: 12624–12627
34 Hashimoto T, Kimura H, Kawamata Y, Maruoka K. *Angew Chem Int Ed*, 2012, 51: 7279–7281
35 Zhang Y, Ao YF, Huang ZT, Wang DX, Wang MX, Zhu J. *Angew Chem Int Ed*, 2016, 55: 5282–5285
36 Zhao W, Huang L, Guan Y, Wulff WD. *Angew Chem Int Ed*, 2014, 53: 3436–3441
37 Zhang J, Yu P, Li SY, Sun H, Xiang SH, Wang JJ, Houk KN, Tan B. *Science*, 2018, 361: eaas8707
38 Zhang J, Lin SX, Cheng DJ, Liu XY, Tan B. *J Am Chem Soc*, 2015, 137: 14039–14042
39 Xu JH, Zheng SC, Zhang JW, Liu XY, Tan B. *Angew Chem Int Ed*, 2016, 55: 11834–11839
40 Zhang LL, Zhang JW, Xiang SH, Guo Z, Tan B. *Chin J Chem*, 2018, 36: 1182–1186
41 Shaabani A, Keshipour S, Shaabani S, Mahyari M. *Tetrahedron Lett*, 2012, 53: 1641–1644
42 Zhang J, Shi W, Liu Q, Chen T, Zhou X, Yang C, Zhang K, Xie Z. *Polym Chem*, 2018, 9: 5566–5571
43 Akiyama T. *Chem Rev*, 2007, 107: 5744–5758
44 Parmar D, Sugiono E, Raja S, Rueping M. *Chem Rev*, 2014, 114: 9047–9153
45 Reid JP, Goodman JM. *Chem Eur J*, 2017, 23: 14248–14260
46 Zhu YI, Stiller MJ. *J Am Acad Dermatol*, 2001, 45: 420–434
47 Beyreuther BK, Freitag J, Heers C, Krebsfänger N, Scharfenecker U, Stöhr T. *CNS Drug Rev*, 2007, 13: 21–42
48 Wehlan H, Oehme J, Schäfer A, Rossen K. *Org Process Res Dev*, 2015, 19: 1980–1986
49 Xie Y, Zhao Y, Qian B, Yang L, Xia C, Huang H. *Angew Chem Int Ed*, 2011, 50: 5682–5686
50 Xu B, Zhu SF, Zhang ZC, Yu ZX, Ma Y, Zhou QL. *Chem Sci*, 2014, 5: 1442–1448